

Full Paper

## **An adaptive radial basis function neural network (RBFNN) control of energy storage system for output tracking of a permanent magnet wind generator**

**Abu H. M. A. Rahim**

Department of Electrical Engineering, King Fahd University of Petroleum and Minerals, Dhahran, Saudi Arabia

Email: [ahrahim@kfupm.edu.sa](mailto:ahrahim@kfupm.edu.sa)

*Received: 10 April 2013 / Accepted: 18 March 2014 / Published: 24 March 2014*

---

**Abstract:** The converters of a permanent magnet synchronous generator have to be properly controlled to achieve maximum transfer of energy from wind. To achieve this goal, this article employs an energy storage device consisting of an energy capacitor interfaced through a voltage source converter which is operated through a smart adaptive radial basis function neural network (RBFNN) controller. The proposed adaptive strategy employs online neural network training as opposed to conventional procedure requiring offline training of a large data-set. The RBFNN controller was tested for various contingencies in the wind generator system. The adaptive online controller is observed to provide excellent damping profile following low grid voltage conditions as well as for other large disturbances. The controlled converter DC capacitor voltage helps maintain a smooth flow of real and reactive power in the system.

**Keywords:** adaptive control, energy storage control, radial basis function neural network, permanent magnet synchronous generator, wind turbine

---

### **INTRODUCTION**

Variable-speed wind turbines based on permanent magnet synchronous generator (PMSG) are found to be attractive in large wind farms because of their advantages in terms of high efficiency of energy production, simple structure, low maintenance, etc. The full-rated converter in the PMSG separates the synchronous generator from the grid, and hence helps easy fault ride-through [1, 2]. However, with increased wind penetration and random wind speed fluctuations, the change in output power can cause grid frequency variations [3]. Maintenance of DC link voltage in the converter system within precise limits is essential for maximum power transfer [4].

Control of the converters of a PMSG for frequency and voltage control has been widely reported in the literature. Two configurations have been considered: the generator-side converter working like a rectifier with the grid-side converter having fully controllable pulse-width-modulated (PWM) system, and the other having full PWM control of both generator-side and grid-side converters [5, 6]. Control of the generator-side converter for maximum power transfer was employed by Rim *et al.* [4], while Haque *et al.* [1] and Muyeen *et al.* [7] used grid-side converters for this purpose. Generator-side and grid-side converters for maximum power transfer and reactive control respectively were reported by Singh *et al.* [8]. Energy storage devices, along with flexible AC transmission system (FACTS), can supply both real (P) and reactive (Q) power and hence can make the converters operate at or near unity power factor. Sharma and Singh [9] and Bhende *et al.* [10] used battery energy storage, along with static compensator (STATCOM), for voltage and frequency control of a PMSG system. A simple proportional-integral-derivative (PID) controller in a STATCOM was shown to improve the stability of a permanent magnet wind generator [11]. Uehere *et al.* [3], Bhende *et al.* [10] and Conroy and Watson [12] demonstrated that coordinated converter control, pitch control, braking resistor and dump load can improve the wind system performance.

With the advancement in intelligent techniques, different families of neural networks have seen a recent rise in application to wind energy control under differing schemes. The use of artificial neural networks for rotor position estimation of a PMSG generator was reported by Batzel and Lee [13]. Lopes [14] employed neural networks for dynamic security assessment of a power system with wind in-feed. Pitch control of a PMSG system was reported using sliding mode control and neural network [15]. Neural network methods employing both back-propagation and radial basis function networks generally depend on training the network with a large set of input-output data. These networks may not perform well under randomly varying wind speed conditions or for the arbitrary nature of disturbances which they are not trained for. For control design, the neural network weights should be computed and updated adaptively according to the system conditions.

This article proposes a novel adaptive radial basis function neural network (RBFNN) control strategy for a permanent magnet wind generator system. The capacitor energy storage system compensates for both real and reactive power requirements of the wind system following any contingency. The weights of the neural network are adapted online from the measurements of the generator outputs. Simulation studies indicate that the adaptive RBFNN control provides excellent damping characteristics even for severe short circuits at the grid bus.

## NOMENCLATURE

$V_w$	Wind speed
$\beta$	Pitch angle
$\lambda$	Tip-speed ratio
$d$ - $q$	Direct and quadrature axes
$R_a$	Stator resistance
$x_d, x_d'$	d-q axes synchronous reactance
$V_s$	Generator stator voltage
$V_t$	Inverter terminal voltage

$V_c, C$	DC capacitor voltage and capacitance in the converter
$V_{dc}, C_{st}$	DC capacitor voltage and capacitance in the storage device
$m_1, m_2$	Modulation indices of converters
$\alpha_1, \alpha_2$	Phase angles of the converters
$\omega_b, \omega$	Base angular speed, rotor angular speed
$H, D$	Inertia constant and damping coefficient
$H_g, H_t$	Inertia constant of generator and turbine
$K_s, \theta_s$	Stiffness constant, torsion angle
$D_b, D_g$	Damping coefficient of turbine and generator
$V_{st}, I_{st}$	Voltage and current of VSC in the storage device
$R_{st}, L_{st}$	Resistance and inductance of VSC
$P_{mech}, P_{elec}$	Mechanical power input, electrical power output
$pu (p.u.)$	Per unit

### PMSG SYSTEM MODEL

The grid-connected permanent magnet generator system considered in this work is shown in Figure 1. Variable frequency voltage generated by the machine is rectified and inverted to grid frequency through fully controlled back-to-back converters located between the generator terminals and the transmission line. A local load and an energy storage unit are connected at the grid side of the inverter. The relationships between the stator voltage, current and flux, expressed in per unit system, are written as [16, 17]:

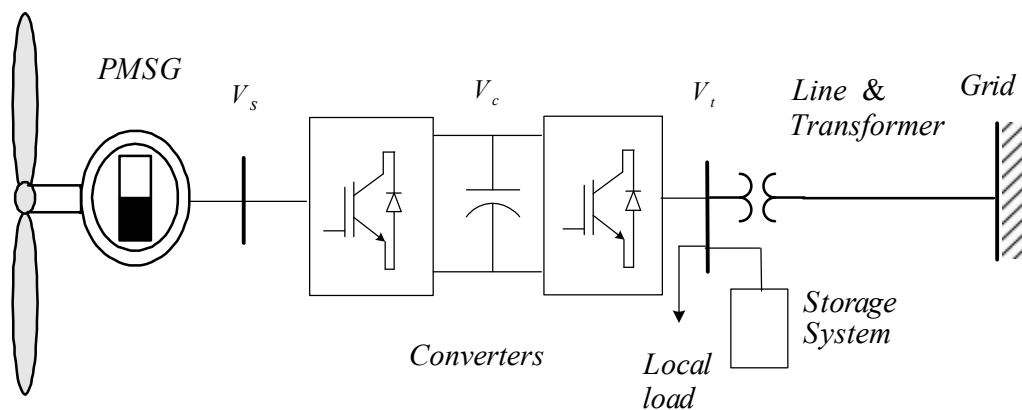


**Figure 1.** Permanent magnet synchronous generator connected to the grid bus

$$\begin{aligned} -R_a I_{sd} - \omega \psi_q + \frac{1}{\omega_o} \frac{d}{dt} (\psi_d) &= V_{sd} \\ -R_a I_{sq} + \omega \psi_d + \frac{1}{\omega_o} \frac{d}{dt} (\psi_q) &= V_{sq} \end{aligned} \quad (1)$$

$$\begin{aligned} \psi_d &= -x_d I_{sd} + \psi_{res} \\ \psi_q &= -x_q I_{sq} \end{aligned} \quad (2)$$

where  $V_s$ ,  $I_s$ , and  $\psi$  are stator voltage, current and flux of the PMSG respectively; subscripts  $d$  and  $q$  represent direct and quadrature axes components of the quantities;  $R_a$ ,  $x_d$  and  $x_q$  are stator resistance and synchronous reactances respectively;  $\psi_{res}$  is the flux from the permanent magnets;  $\omega$  and  $\omega_0$  are generator angular frequency and base angular frequency respectively.

The electromechanical equations of motion of the generator and turbine rotor are written in terms of their respective angular speeds ( $\omega$ ,  $\omega_t$ ) as:

$$\begin{aligned} \dot{\omega} &= \frac{1}{2H_g} (K_s \theta_s - P_{elec} - D_g (\omega - 1)) \\ \dot{\omega}_t &= \frac{1}{2H_t} (P_{mech} - K_s \theta_s - D_t (\omega_t - 1)) \\ \dot{\theta}_s &= \omega_0 (\omega_t - \omega) \end{aligned} \quad (3)$$

where  $H$  and  $D$  are, respectively, inertia constants and damping coefficients of turbine and generator;  $K_s$  and  $\theta_s$  represent, respectively, stiffness coefficient and torsion angle of the shaft connecting the two masses. The expressions for mechanical input power  $P_{mech}$ , which is the wind turbine output, and electrical power output  $P_{elec}$  are:

$$\begin{aligned} P_{mech} &= \frac{1}{2} \alpha A_b C_{pw} (\gamma, \beta) V_\omega^3 \\ P_{elec} &= \psi_{res} I_{sq} + (x_q - x_d) I_{sd} I_{sq} \end{aligned} \quad (4)$$

where  $\alpha$ ,  $A_b$ ,  $C_{pw}$ ,  $\gamma$  and  $\beta$  are density of air, turbine blade swept area, power coefficient, tip-speed ratio and turbine pitch angle respectively.

The normalised differential equation relating the inverter current ( $I_i$ ) to the internal voltage ( $V_i$ ) and terminal voltage ( $V_t$ ) can be broken up in terms of d-q quantities as:

$$\begin{aligned} \frac{dI_{id}}{dt} &= \frac{\omega_0}{x_i} [V_{id} - V_{td} - R_i I_{id} + \omega x_i I_{iq}] \\ \frac{dI_{iq}}{dt} &= \frac{\omega_0}{x_i} [V_{iq} - V_{tq} - R_i I_{iq} - \omega x_i I_{id}] \end{aligned} \quad (5)$$

where subscripts  $d$  and  $q$  refer to direct and quadrature axes components of the inverter voltage and current;  $R_i$  and  $x_i$  are inverter resistance and reactance respectively. The generator stator voltage ( $V_s$ ) and inverter internal voltage ( $V_i$ ) are related to the DC capacitor voltage ( $V_c$ ), converter and inverter modulation indices ( $m_1$ ,  $m_2$ ) and phase angles ( $\alpha_1$ ,  $\alpha_2$ ) through:

$$\begin{aligned} V_s &= m_1 V_c \angle \alpha_1 \\ V_i &= m_2 V_c \angle \alpha_2 \end{aligned} \quad (6)$$

The equation of the DC link capacitor located between the two converters is derived from the condition that the power supplied by the rectifier equals the power input to the inverter, and is expressed as:

$$\frac{dV_c}{dt} = \frac{1}{C} [m_1 I_{sd} \cos \alpha_1 + m_1 I_{sq} \sin \alpha_1 - m_2 I_{id} \cos \alpha_2 - m_2 I_{iq} \sin \alpha_2] \quad (7)$$

A full list of symbols is included in the nomenclature section.

### ENERGY STORAGE CONTROLLER MODEL

The circuit configuration of the energy storage device is shown in Figure 2. It contains a storage capacitor which is interfaced to the wind generator system through a voltage source converter (VSC) and a buck-boost converter operated through switches  $S_1$  and  $S_2$  [18]. By controlling the delay angle of the switches in the converter, the direction of power flow can be reversed. The modulation index of the VSC allows control of the internal voltage given by the relation  $V_{st} = mV_{dc} \angle \psi + \theta_m$ . Here,  $\theta_m$  is the angle of the inverter terminal voltage  $V_t$  at the point of connection of the storage device. A combination of modulation index and phase angle ( $m, \psi$ ) control allows control of real and reactive power injection to the wind system. Applying Kirchoff's voltage law, the dynamic relationship for  $d$ - $q$  components of VSC output currents can be written as:

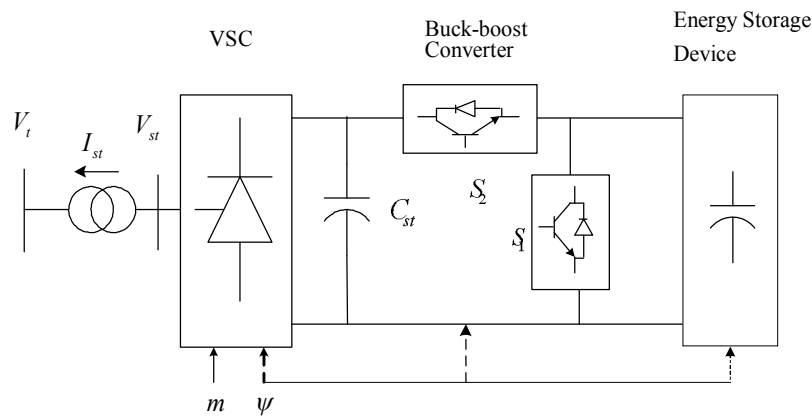


**Figure 2.** Capacitor energy storage control system

$$\begin{aligned} \frac{dI_{std}}{dt} &= \frac{\omega_0}{L_{st}} [-R_{st} i_{std} + \omega L_{st} I_{stq} + mV_{dc} \cos(\psi + \theta_m) - V_{td}] \\ \frac{dI_{stq}}{dt} &= \frac{\omega_0}{L_{st}} [-\omega L_{st} I_{std} + R_{st} I_{stq} + mV_{dc} \sin(\psi + \theta_m) - V_{tq}] \end{aligned} \quad (8)$$

where  $I_{std}$  and  $I_{stq}$  are, respectively, the direct and quadrature axes components of STATCOM current  $I_{st}$ ;  $V_{td}$  and  $V_{tq}$  are the  $d$ - $q$  components respectively of terminal voltage  $V_t$ ;  $V_{dc}$  represents the voltage across the DC capacitor  $C_{st}$ ;  $R_{st}$  and  $L_{st}$  are the effective resistance and inductance of the VSC respectively. The voltage equation for DC link capacitor in the storage system, obtained by following the same procedure as in (8), is written as:

$$\frac{dV_{dc}}{dt} = \frac{-m}{C_{st}} [I_{std} \cos(\psi + \theta_m) + I_{stq} \sin(\psi + \theta_m)] + \frac{I_{ces}}{C_{st}} \quad (9)$$

The current from the storage capacitor ( $I_{ces}$ ) is related to capacitance and its voltage ( $V_{ces}$ ) by a simple relationship:

$$\frac{dV_{ces}}{dt} = \frac{I_{ces}}{C_{es}} \quad (10)$$

Combining the dynamic equations (1), (3), (5), (7), (8), (9) and (10), and eliminating the non-state variables through appropriate relationships, the composite state model for the PMSG system, along with the storage control device, is expressed as:

$$\begin{aligned} \dot{x} &= f[x, u] \\ y &= g[x, u] \end{aligned} \quad (11)$$

The control vector ( $u$ ) is composed of  $m$  and  $\psi$  of the energy storage device and  $y$  represents the vector of chosen outputs.

### ADAPTIVE RBFNN CONTROLLER

The main concept of the proposed control design is to maintain the wind generator output to pre-specified values following wind speed change, low voltage conditions or other arbitrary disturbances in the system. The controls in the storage system are activated by neural network controllers to compensate for P and Q imbalance in the wind system. In the usual neural network applications the offline training of large amounts of input-output data is required to generate a weighting matrix. These weights may not predict the output accurately in randomly or arbitrarily changing system conditions. For satisfactory control estimates, the training should be done online and the weight updates should be made as time progresses [19].

The configuration of the adaptive neural network controller proposed in this study is shown in Figure 3. The controller consists of a core radial basis function network (RBFN), an adaptation system for the RBFN and a proportional stabilising controller. The adaptation system consists of a linear estimate of the system matrices, an adaptation algorithm and a weight update policy. A proportional stabilising controller is incorporated in the strategy to ensure that the RBFN controller initialisation is stable while the weighting updates are initiated. Both the RBFN and the stabilising controller are activated by an error signal between the reference input ( $r$ ) and the actual output ( $y$ ). The output from the adapted neural network, along with the stabilising controller, is then fed to the wind generator system. As the training proceeds, the RBFN takes over the stabilising proportional controller [20, 21].

The structure of the RBFNN is shown in Figure 4. The neurons in the radial basis networks usually have three layers: the input, the hidden and the output layers. At any time, step  $k$ , the output of the hidden layer, can be expressed through [22]:

$$V(k) = W(k)^T \Psi(k) \quad (12)$$

where  $W$  is the weight matrix and  $\Psi$  is a set of basis functions, the  $j^{th}$  kernel of which is usually chosen to be the Gaussian function:

$$\psi_j(k) = \exp\left(-\frac{\|r(k) - c_j\|^2}{\sigma_j^2}\right) \quad (13)$$

where  $c_j$  is the centre of the  $j^{th}$  neuron and  $\sigma_j$  represents the width of the layer.

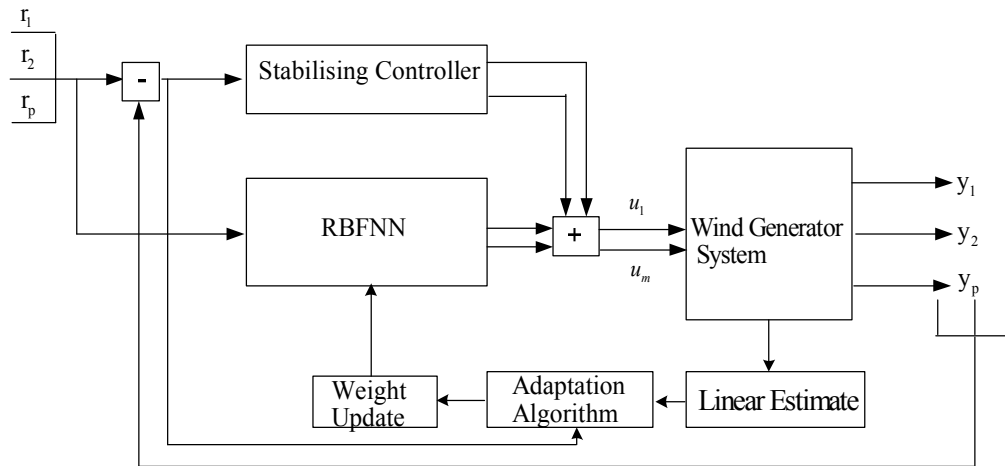


**Figure 3.** RBFN-based adaptive controller for wind generator system

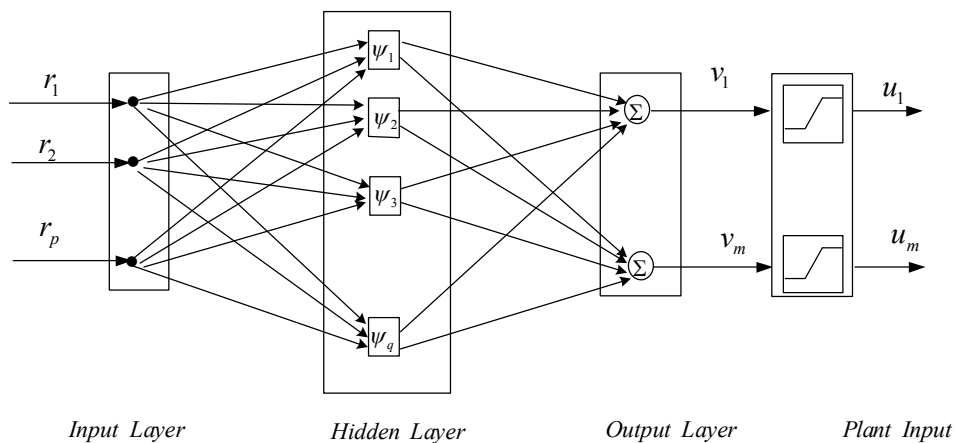


**Figure 4.** RBFNN structure

Considering the saturation to be a tangent sigmoid function, the  $j^{th}$  component of input ( $u$ ) to the plant can be expressed as:

$$u_j(k) = \alpha_1 \frac{e^{\beta v_j(t)} - 1}{e^{\beta v_j(t)} + 1} = \alpha_1 \frac{e^{\beta w_j^T \phi(k)} - 1}{e^{\beta w_j^T \phi(k)} + 1} \quad (14)$$

Here  $u_{max} = u_{min} = \alpha_1$ , and  $\beta_1$  is slope of the sigmoid function. The error function ( $e$ ) is defined as:

$$e(k) = r(k) - y(k) \quad (15)$$

The weighting matrix is obtained by minimising the mean square error ( $E$ ), which is the product of the transpose of error ( $e^T$ ) and error  $e$  at any time step  $k$ :

$$E = e^T(k) e(k) \quad (16)$$

The update law for the elements of the weighting matrix  $W(k)$ , using the gradient descent technique, is written as:

$$w_j(k+1) = w_j(k) - \eta \frac{\partial E}{\partial w_j} \quad (17)$$

After linearisation of the system of equations (11), its discrete form can be written in terms of A, B, C, D matrices as:

$$\begin{aligned} x(k+1) &= Ax(k) + Bu(k) \\ y(k) &= Cx(k) + Du(k) \end{aligned} \quad (18)$$

Substituting output  $y$  from (18) gives the expression for the gradient as:

$$\frac{\partial E}{\partial w_j} = -2e^T(k) \frac{\partial}{\partial w_j} [Cx(k) + Du(k)] \quad (19)$$

Using the chain rule and substituting the state equation from (18), it can be shown that:

$$\frac{\partial E}{\partial w_j} = -2e^T(k) \left[ \frac{\partial CBu(k-1)}{\partial w_j} + \frac{\partial Du(k)}{\partial u_j} \right] \quad (20)$$

The recursive formula for the update of the weights is then:

$$\begin{aligned} w_j(k+1) &= w_j(k) + 2\eta \sum_{l=1}^p e_l(k) \\ &\quad \left\{ \phi_{lj} \alpha_1 \frac{2\beta_1(k-1)e^{\beta_1 w_j^T(k-1)}}{(e^{\beta_1 w_j^T(k-1)} + 1)^2} + D_{lj} \alpha_1 \frac{2\beta_1(k)e^{\beta_1 w_j^T(k)}}{(e^{\beta_1 w_j^T(k)} + 1)^2} \right\} \end{aligned} \quad (21)$$

In the above equation,  $p$  is the number of output and  $\phi_{lj}$  is the  $lj^{\text{th}}$  element of  $(CB + \lambda_l)$  matrix. The quantity  $\lambda_l$  is selected so as to overcome zero entries of matrix  $CB$  at the start of the training process [23]. Quantity  $\eta$  is the learning rate of the radial basis function network. A step-by-step process is tabulated in Algorithm 1.

---

#### Algorithm 1. Adaptive RBFNN control algorithm

---

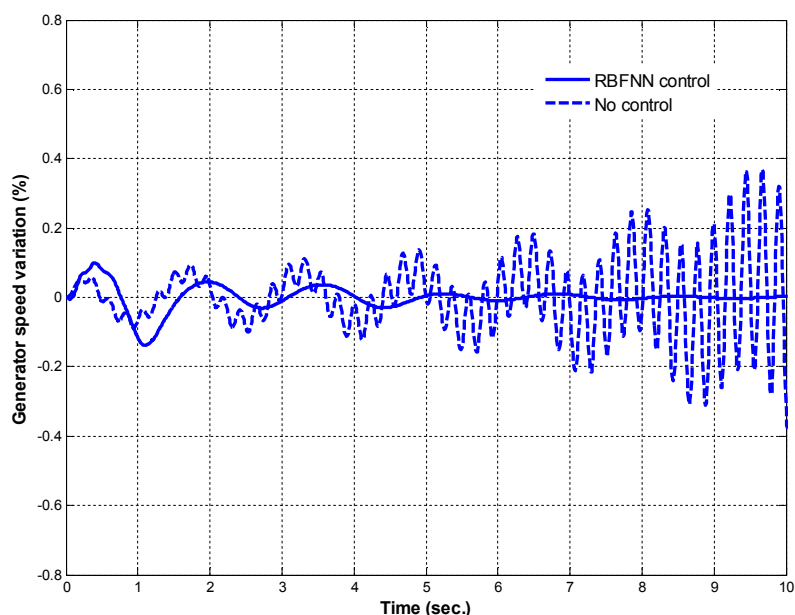
- Obtain a linear estimate of the PMSG model using offline identification or linearisation of the non-linear model.
  - Initialise stabilising controller with a gain small enough to ensure a stable initialisation.
  - Initialise RBFNN with random synaptic weights having small values.
  - Initialise a small learning rate  $\eta$ .
  - Select  $\alpha$  depending upon the constraints required on the control inputs.
  - Based on (22), the weights are updated as the PMSG outputs are acquired at each sampling instance.
  - If the learning rate is small enough for the weights to converge, the PMSG outputs follow the reference trajectory.
- 

#### TESTING THE CONTROLLER

The adaptive RBFNN controller design was implemented on the permanent magnet generator system considered in Figure 1. The control inputs are the modulation index and phase angles of the storage system converters, while the outputs to be tracked are the generator speed and terminal

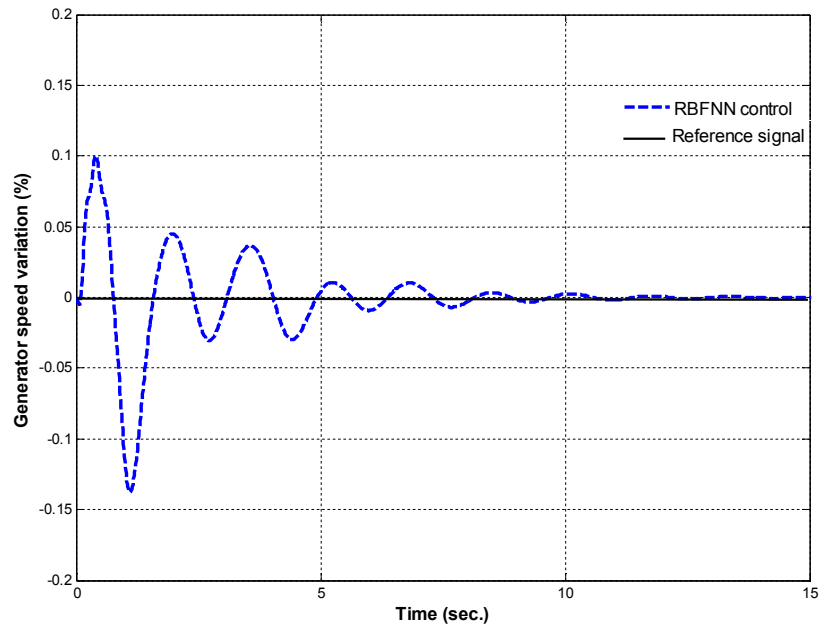
voltage. The generator is considered to be delivering 0.95 per unit (pu) power under steady condition at an average wind speed of 12 m/sec. The damping of the turbine-generator rotor is considered to be zero for a worst-case scenario. The system parameters are included in the Appendix. Only those disturbances which give rise to oscillatory or unstable responses are reported in this article.

Figure 5 shows the synchronous generator speed variation when it is subjected to a 20% input torque pulse on the shaft for 300 milliseconds (ms). The torque unbalance gives an oscillatory response in the generator because of zero damping. Although the converter and DC capacitor system isolate the two synchronous systems, the generator and the grid, part of the large oscillations in the generator will get past the converters into the grid. From the response shown in the Figure, it can be seen that the adaptive online RBFN controller results in larger overshoots compared to the uncontrolled case at the beginning of the adaptive training process. This is due to near-zero initialisation of the RBF weights. As time progresses the network gets trained and the oscillations die out quickly.



**Figure 5.** Speed variation of permanent magnet synchronous generator following a 20% input torque pulse for 300 ms with and without proposed RBFNN control

Figure 6 shows a comparison of the speed of the synchronous generator with the reference value when RBFNN control is applied. Figure 7 shows that the sum of squared error converges very fast. Figure 8 shows that in the early part of the transients, when the network has not been properly trained, the generator stator current momentarily increases by about 25%. However, it quickly returns to the normal level as the neural network gets trained. Maintenance of a constant level of the DC-link capacitor voltage is essential for maximising the power transfer through the converters. It can be observed from Figure 9 that the DC link voltage recovery is very fast with the adaptive neural network control. Variations of the control variables ( $m$  and  $\psi$ ), given in Figure 10, show that the control effort falls to a reasonably smaller value quickly after a slightly large excursion at the start of the training process.



**Figure 6.** Variation of controlled generator speed from reference value

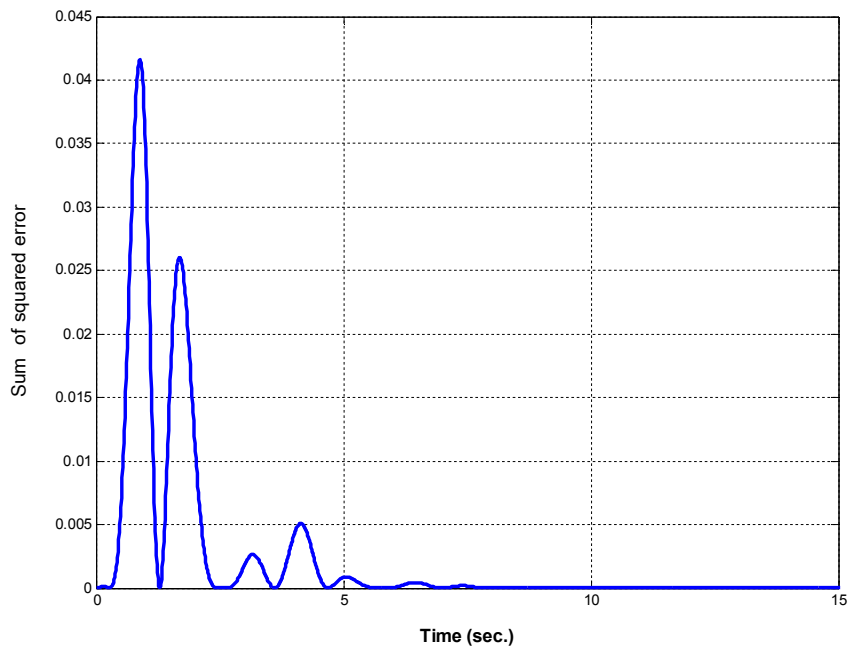


**Figure 7.** Sum of squared error for 20% input torque pulse

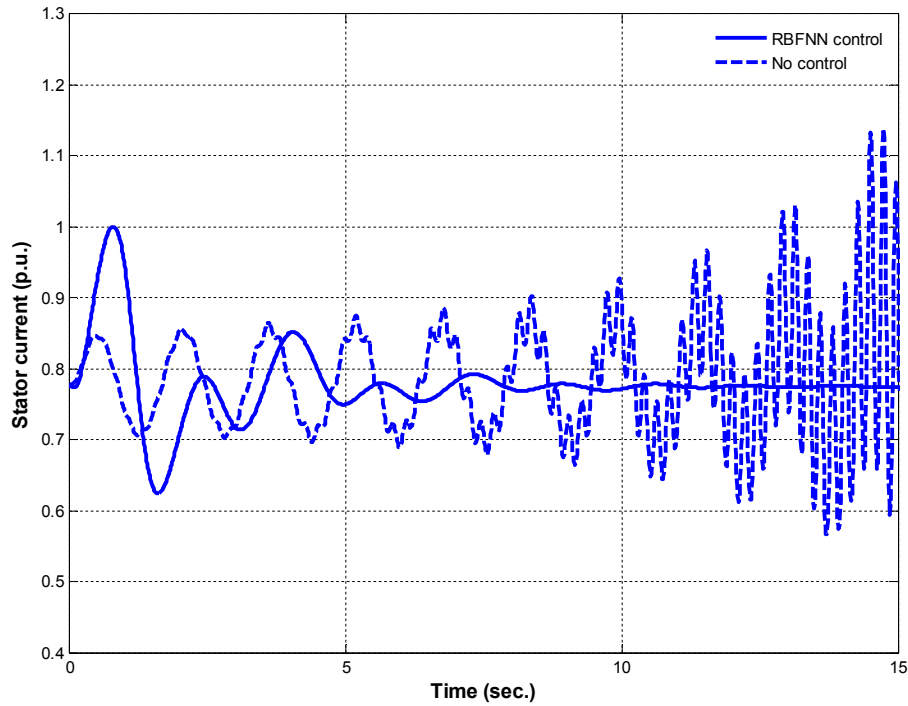


**Figure 8.** Generator stator current variation with and without adaptive RBFNN control

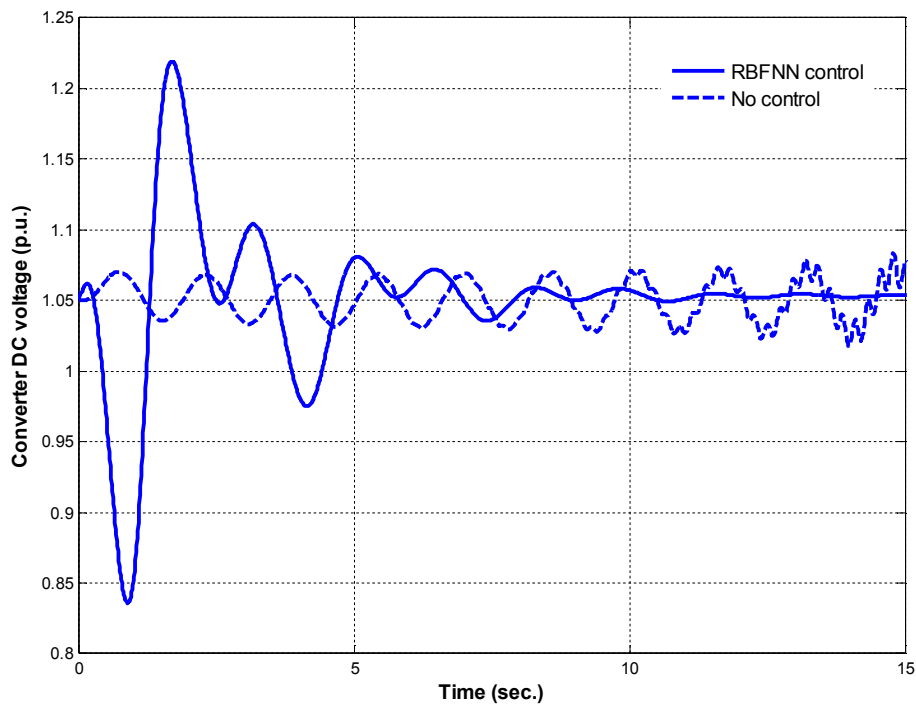


**Figure 9.** Converter DC-link voltage variation following a 20% input torque pulse

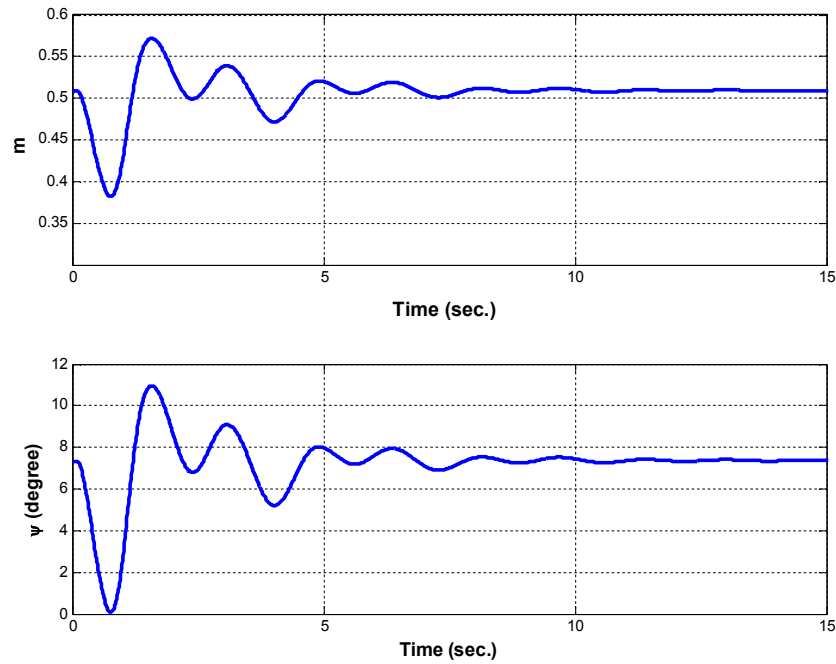


**Figure 10.** Modulation index (top figure) and phase angle controls (bottom figure) generated for 20% torque pulse case

Figure 11 shows a comparison of the generator speed variation response obtained from the following two strategies: a) the proposed adaptive RBFNN control, and b) decoupled P-Q strategy of supercapacitor control as reported in the literature [18]. The decoupled supercapacitor control of the PMSG involves a relatively complex controller, whose parameters are designed through an optimisation procedure. The major advantage of the proposed RBFNN controller over the earlier reported work is that the former can be implemented online and its performance is robust.

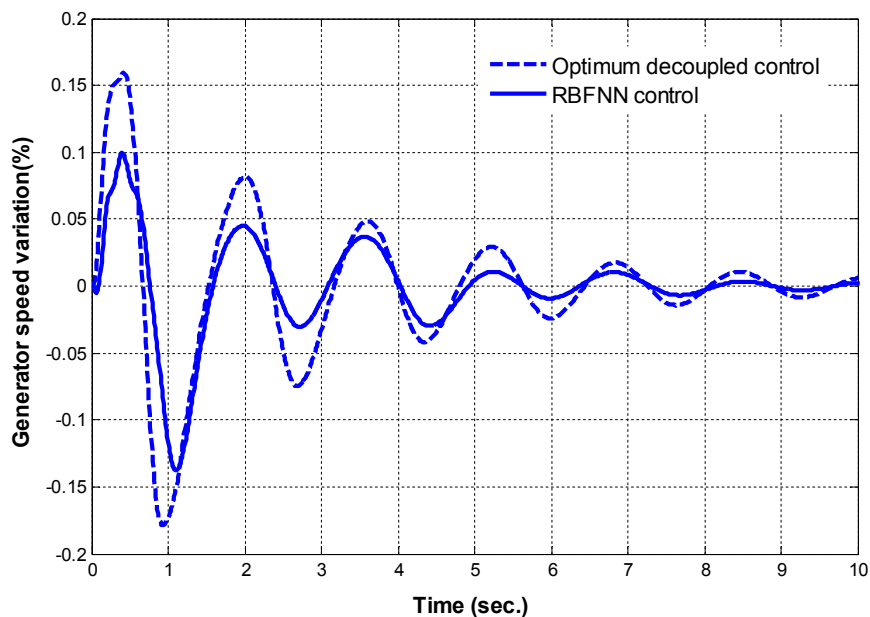


**Figure11.** Comparison of generator speed variation obtained from proposed RBFNN control with optimum de-coupled P-Q strategy reported in the literature

The robustness of the RBFNN controller was tested at very low voltage conditions on the grid bus. Figures 12-13 show variations in the turbine speed and converter DC voltage respectively, following a 200-ms three-phase fault on the grid. The system response without any additional control results in growing oscillation. The RBFNN strategy controls the oscillation effectively and restores normal operation in less than 10 sec. The initial generator current and converter voltage show large peaks because of random initialisation of the weights. However, as time progresses the weights get trained and the system response reaches steady value smoothly.

Figure 14 shows the variation in wind turbine speed and the generator terminal voltage following repetitive disturbances by input torque pulse. As can be observed, the initial transients in the subsequent disturbance are not as pronounced under the RBFNN control since the weight initialisation is no longer needed.

From a number of simulation studies, it is observed that the proposed adaptive RBFNN restores even the dynamically unstable system to normal operation very quickly. The amount of control required to achieve this has been observed to be reasonably small. The adaptive strategy is simple to implement as it involves only a few steps of computation.

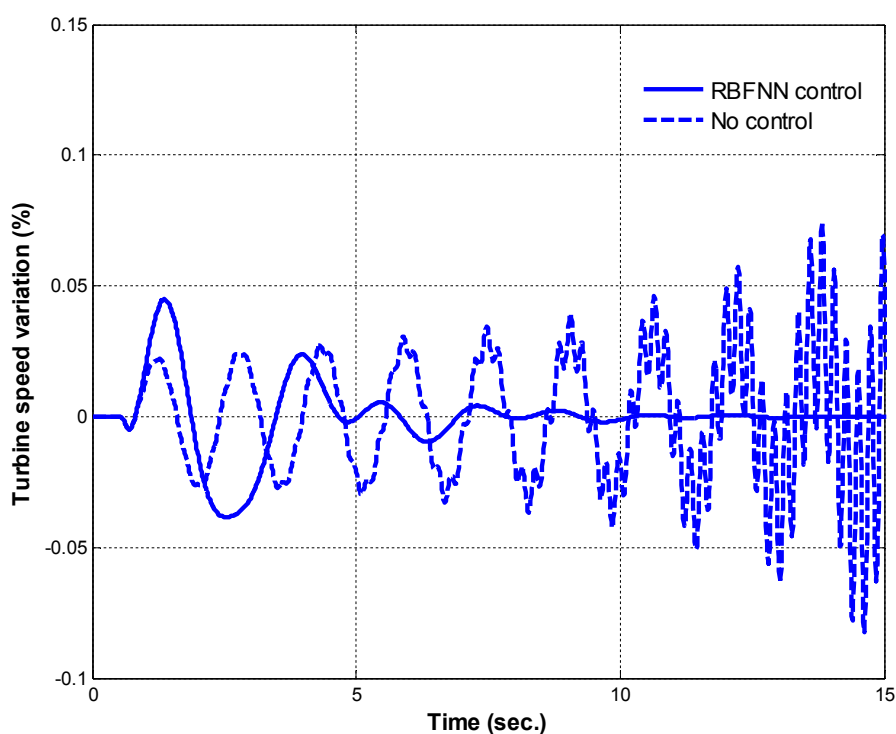


**Figure 12.** Wind turbine speed variation following a 200-ms three-phase fault at the grid bus with and without adaptive controller

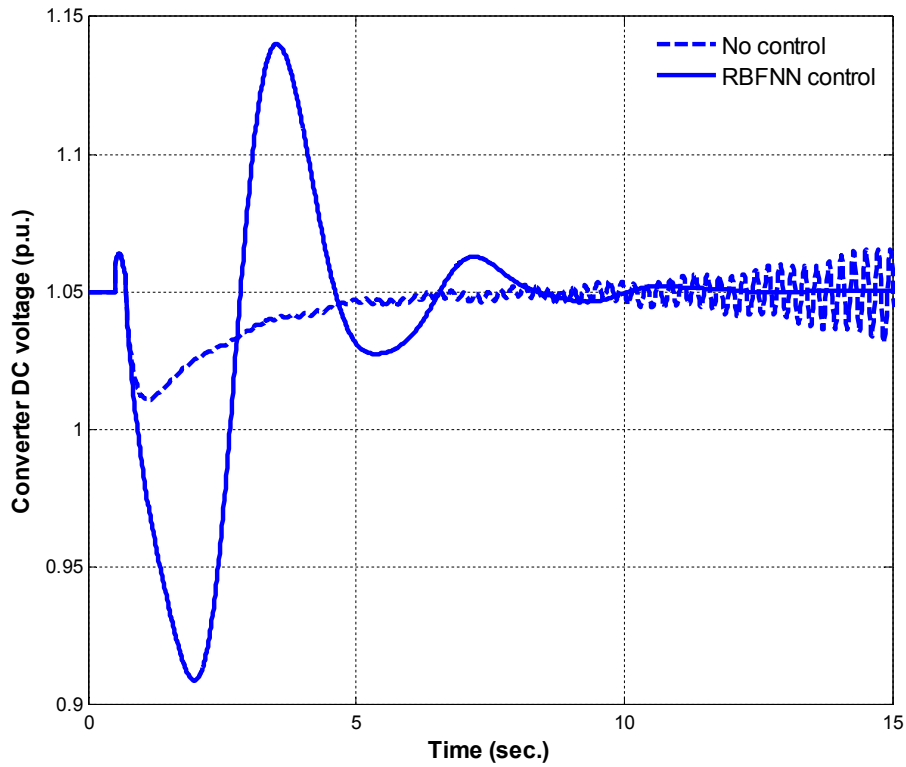


Figure 13. Converter DC voltage variation following a 200-ms grid fault corresponding to Fig. 12

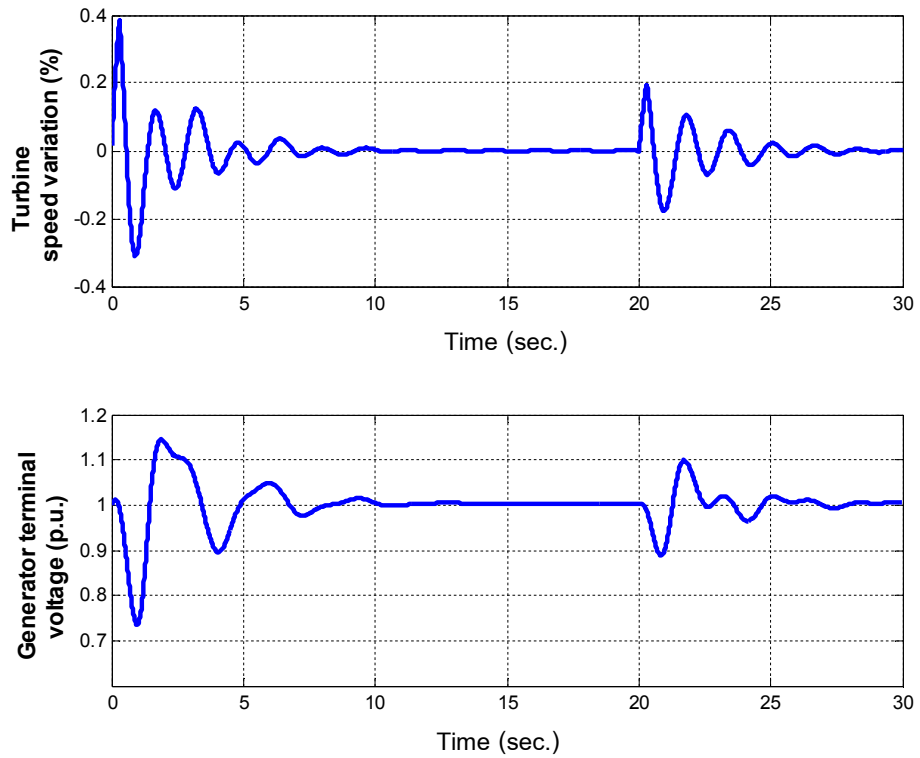


Figure 14. Wind turbine speed variation and generator terminal voltage under RBFNN control when subjected to repetitive disturbances

## CONCLUSIONS

A novel online adaptive control strategy for an energy storage device has been proposed using artificial neural network. The strategy employs selected system outputs to predict the control and also updates the network weights online. No offline training is involved in the process. The objective of the strategy is to restore the permanent magnet wind generator to pre-specified levels of output following arbitrary disturbances in the system. This has been achieved by compensating for the wind generator P and Q imbalance through the energy storage device. The radial basis function considered has fast convergence characteristics. The proposed adaptive neural network control strategy is much superior to the classical neural controls, which employ fixed weights.

## ACKNOWLEDGEMENTS

This work was conducted under KFUPM Research Group Project #RG1202-1&1202-2. The author wishes to acknowledge the support of King Fahd University of Petroleum and Minerals. Syed Z. Rizvi, lecturer of electrical engineering, is specially acknowledged for his contribution in the computational part.

## REFERENCES

1. M. E. Haque, M. Negnevitsky and K. M. Muttaqi, "A novel control strategy for a variable-speed wind turbine with permanent-magnet synchronous generators", *IEEE Trans. Ind. Appl.*, **2010**, *46*, 331-339.
2. S. Zhang, K. J. Tseng, D. M. Vilathgamuwa, T. D. Nguyen and X. Y. Wang, "Design of a robust grid interface system for PMSG-based wind turbine generators", *IEEE Trans. Ind. Electron.*, **2011**, *58*, 316-328.
3. A. Uehara, A. Pratap, T. Goya, T. Senjyu, A. Yona, N. Urasaki and T. Funabashi, "A coordinated control method to smooth wind power fluctuations of a PMSG-based WECS", *IEEE Trans. Energy Convers.*, **2011**, *26*, 550-558.
4. K. H. Kim, Y. C. Jeung, D. C. Lee and H. G. Kim, "LVRT scheme of PMSG wind power systems based on feedback linearization", *IEEE Trans. Power Electron.*, **2012**, *27*, 2376-2384.
5. S. Kato and M. Michihira, "A comparative study on power generation characteristics of permanent magnet synchronous generators", Proceedings of International Power Electronics Conference, **2010**, Sapporo, Japan, pp.1499-1505.
6. S. Li, T. A. Haskew and L. Xu, "Conventional and novel control designs for direct driven PMSG wind turbines", *Electr. Power Syst. Res.*, **2010**, *80*, 328-338.
7. S. M. Mueen, R. Takahashi, T. Murata, J. Tamura, M. H. Ali, Y. Matsumura, A. Kuwayama and T. Matsumoto, "Low voltage ride through capability enhancement of wind turbine generator system during network disturbance", *IET Renew. Power Gener.*, **2009**, *3*, 65-74.
8. M. Singh, V. Khadkikar and A. Chandra, "Grid synchronisation with harmonics and reactive power compensation capability of a permanent magnet synchronous generator-based variable speed wind energy conversion system", *IET Power Electron.*, **2011**, *4*, 122-130.
9. S. Sharma and B. Singh, "Control of permanent magnet synchronous generator-based stand-alone wind energy conversion system", *IET Power Electron.*, **2012**, *5*, 1519-1526.
10. C. N. Bhende, S. Mishra and S. G. Malla, "Permanent magnet synchronous generator-based standalone wind energy supply system", *IEEE Trans. Sust. Energy*, **2011**, *2*, 361-373.

11. L. Wang and D. N. Truong, "Dynamic stability improvement of four parallel-operated PMSG-based offshore wind turbine generators fed to a power system using a STATCOM", *IEEE Trans. Power Del.*, **2013**, 28, 111-119.
12. J. Conroy and R. Watson, "Aggregate modelling of wind farms containing full-converter wind turbine generators with permanent magnet synchronous machines: Transient stability studies", *IET Renew. Power Gener.*, **2009**, 3, 39-52.
13. T. D. Batzel and K. Y. Lee, "High resolution rotor angle estimation for permanent magnet synchronous machines with Hall effect position sensors using neural networks", *Int. J. Eng. Intelli. Syst. Elect. Eng. Comm.*, **2000**, 8, 59-65.
14. J. A. P. Lopes, "Application of artificial neural networks to dynamic security assessment of electric power systems", *Int. J. Eng. Intelli. Syst. Elect. Eng. Comm.*, **1999**, 7, 19-28.
15. W. M. Lin, C. M. Hong, T. C. Ou and T. M. Chiu, "Hybrid intelligent control of PMSG wind generation system using pitch angle control with RBFN", *Energy Convers. Manage.*, **2011**, 52, 1244-1251.
16. S. Miyabukuro, M. Takiguchi, R. Takahashi, T. Murata, J. Tamura and T. Tsuchiya, "Modeling and simulation of wind turbine-fed interior permanent magnet synchronous generator", Proceedings of 18<sup>th</sup> International Conference on Electrical Machines, **2008**, Vilamoura, Portugal, pp.1-6.
17. A. O. D. Tommaso, R. Miceli, G. R. Galluzzo and M. Trapanese, "Efficiency maximization of permanent magnet synchronous generators coupled to wind turbines", Proceedings of IEEE Power Electronics Specialist Conference, **2007**, Orlando (FL), USA, pp.1267-1272.
18. A. H. M. A. Rahim, "Modeling and control of a PMSG wind system with STATCOM capacitor energy storage device", Proceedings of 12<sup>th</sup> IASTED Conference on Modelling and Simulation, **2012**, Banff, Canada, pp.249-254.
19. S. Kamalasan and A. A. Ghandakly, "A neural network parallel adaptive controller for dynamic system control", *IEEE Trans. Instr. Measur.*, **2007**, 56, 1786-1796.
20. M. T. Hagan, H. B. Demuth and O. D. Jesus, "An introduction to the use of neural networks in control systems", *Int. J. Robust Nonlinear Contr.*, **2002**, 12, 959-985.
21. J. Sarangapani, "Neural Network Control of Nonlinear Discrete-Time Systems", CRC Press, Boca Raton (FL), **2006**, Ch.3.
22. S. Huang, K. K. Tan, T. H. Lee and A. S. Putra, "Adaptive control of mechanical systems using neural networks", *IEEE Trans. Syst. Man Cyber. Part C*, **2007**, 37, 897-903.
23. H. N. Al-Duwaish and S. Z. Rizvi, "A robust controller for non-linear MIMO systems using radial basis function neural network", *Proc. IMechE Part I: J. Syst. Contr. Eng.*, **2011**, 225, 667-682.

**APPENDIX****System Data (in per unit, except stated otherwise)**

*PMSG quantities:* 1.5 MVA, 690 V, 40-pole,  $f_b = 11.5$  Hz,  $R_a = 0.01$ ,  $X_d = 1$ ,  $X_q = 0.7$ ,  $H_g = 0.5$ s,  $H_t = 3$ s,  $K_s = 0.3$ , Residual flux = 0.9

*Converter parameters:*  $R_i = 0.05$ ,  $X_i = 0.1$ ,  $C = 1$ ; Storage capacitor and VSC: 250 kW,  $R_{st} = 0.01$ ,  $L_{st} = 0.15$ ,  $C_{dc} = 1$

*Local load and line:*  $P = 200$  kW,  $Q = 400$  kVAR (including capacitor);  $R_{line} = 0.1$ ,  $X_{line} = 0.2$